

# miR-135b Stimulates Osteosarcoma Recurrence and Lung Metastasis via Notch and Wnt/ $\beta$ -Catenin Signaling

Hua Jin,<sup>1,7</sup> Song Luo,<sup>2,7</sup> Yun Wang,<sup>3,7</sup> Chang Liu,<sup>4</sup> Zhenghao Piao,<sup>5</sup> Meng Xu,<sup>2</sup> Wei Guan,<sup>6</sup> Qing Li,<sup>6</sup> Hua Zou,<sup>6</sup> Qun-You Tan,<sup>6</sup> Zhen-Zhou Yang,<sup>6</sup> Yan Wang,<sup>2</sup> Dong Wang,<sup>6</sup> and Cheng-Xiong Xu<sup>6</sup>

<sup>1</sup>Department of Thoracic Surgery, Daping Hospital and Research Institute of Surgery, Third Military Medical University, Chongqing 400042, China; <sup>2</sup>Department of Orthopaedics, The General Hospital of Chinese People's Liberation Army, Beijing 100853, China; <sup>3</sup>Department of Pathology, The General Hospital of Chinese People's Liberation Army, Beijing 100853, China; <sup>4</sup>Department of Biochemistry and Molecular Biology, School of Basic Medical Sciences, Jilin University, Changchun 130021, China; <sup>5</sup>Department of Basic Medical Science, School of Medicine, Hangzhou Normal University, Hangzhou 310036, China; <sup>6</sup>Cancer Center, Daping Hospital and Research Institute of Surgery, Third Military Medical University, Chongqing 400042, China

**Cancer stem cells (CSCs) play an important role in osteosarcoma (OS) metastasis and recurrence, and both Wnt/ $\beta$ -catenin and Notch signaling are essential for the development of the biological traits of CSCs. However, the mechanism that underlies the simultaneous hyperactivation of both Wnt/ $\beta$ -catenin and Notch signaling in OS remains unclear. Here, we report that expression of miR-135b correlates with the overall and recurrence-free survival of OS patients, and that miR-135b has an activating effect on both Wnt/ $\beta$ -catenin and Notch signaling. The overexpression of miR-135b simultaneously targets multiple negative regulators of the Wnt/ $\beta$ -catenin and Notch signaling pathways, including glycogen synthase kinase-3 beta (GSK3 $\beta$ ), casein kinase 1a (CK1 $\alpha$ ), and ten-eleven translocation 3 (TET3). Therefore, upregulated miR-135b promotes CSC traits, lung metastasis, and tumor recurrence in OS. Notably, antagonizing miR-135b potently inhibits OS lung metastasis, cancer cell stemness, CSC-induced tumor formation, and recurrence in xenograft animal models. These findings suggest that miR-135b mediates the constitutive activation of Wnt/ $\beta$ -catenin and Notch signaling, and that the inhibition of miR-135b is a novel strategy to inhibit tumor metastasis and prevent CSC-induced recurrence in OS.**

## INTRODUCTION

Osteosarcoma (OS) is the most common primary malignant tumor in children and adolescents.<sup>1</sup> The overall 5-year survival rate of patients with OS is ~70%, but 30% of patients with OS do not survive for more than 5 years.<sup>2</sup> The treatment of patients with OS often fails because of the development of chemoresistance, metastasis,<sup>3</sup> and disease recurrence.<sup>4</sup> A total of 20% of OS patients present with lung metastasis at diagnosis, and OS recurs in 30%–40% of patients who are initially diagnosed with non-metastatic disease.<sup>5</sup> The most common site of relapse in patients with OS was the lung,<sup>5</sup> and the long-term survival rate of patients with recurrent OS was less than 20%;<sup>6</sup> even current aggressive treatments do not guarantee long-term survival.<sup>7</sup> Thus, the elucidation of the mechanisms that underlie metastatic recurrence

is fundamental for the development of novel therapeutic treatments for OS.

Accumulating evidence suggests that cancer stem cells (CSCs) may be responsible for therapy resistance, metastasis, and recurrence. CSCs are a small subset of cells within a tumor that have the ability to self-renew.<sup>8</sup> They can regenerate all of the cell types within the tumor, which results in cancer recurrence.<sup>9</sup> Therefore, the CSC is emerging as an important therapeutic target for anticancer therapies. Recent data demonstrate that OS also contains a self-renewing cell population exhibiting a stem-like phenotype and highly resistant to current therapies, and it is implicated in tumor recurrence and metastasis in OS.<sup>10–14</sup> CSC development and the maintenance of its “stemness” are associated with aberrations in several molecular cascades.<sup>15</sup> Studies have shown that activation of Notch and Wnt/ $\beta$ -catenin signaling is essential for the CSC development and maintenance in OS.<sup>16–20</sup> Thus, an understanding of the biological basis for the observed deregulation (i.e., hyperactivation) of Wnt/ $\beta$ -catenin and Notch signaling is of great value for the future development of novel therapeutic strategies of OS. Interestingly, studies show that Wnt/ $\beta$ -catenin and Notch signaling were simultaneously activated in CSCs,<sup>21</sup> but the mechanism still is not fully understood.

miRNAs comprise a class of small non-coding RNAs that negatively regulate the expression of target genes at the post-transcriptional level through interaction with the 3' UTRs of the target genes.<sup>22</sup> Recent studies have shown that hyperactivation of the Notch or

Received 1 November 2016; accepted 12 June 2017;  
<http://dx.doi.org/10.1016/j.omtn.2017.06.008>.

<sup>7</sup>These authors contributed equally to this work.

**Correspondence:** Cheng-Xiong Xu, Daping Hospital and Research Institute of Surgery, Third Military Medical University, 10 Changjiang Zhilu, Daping, Yuzhong District, Chongqing 400042, China.

**E-mail:** [xuchengxiong@hanmail.net](mailto:xuchengxiong@hanmail.net)

Wnt/ $\beta$ -catenin pathways in tumors is partly associated with the dysregulation of certain microRNAs (miRNAs) that in turn regulate the Notch or Wnt/ $\beta$ -catenin pathways.<sup>23,24</sup> Aberrantly regulated expression of miR-135b has been detected in several types of tumors including OS.<sup>25,26</sup> Interestingly, although not in tumors, upregulated miR-135b results in the activation of Wnt/ $\beta$ -catenin signaling in glomerulopathies.<sup>27</sup> In addition, according to a report, activated Wnt/ $\beta$ -catenin signaling is sufficient to activate the Notch pathway in osteocytes.<sup>28</sup> Based on these findings, we propose that aberrantly regulated expression of miR-135b in OS may be involved in the development of CSCs and in the maintenance of stemness, and might therefore affect OS metastasis and recurrence.

Here, we demonstrated that the overexpression of miR-135b is closely associated with OS metastasis of the lung, recurrence, and poor patient survival. miR-135b is also functionally linked to the activation of the Notch and Wnt/ $\beta$ -catenin pathways via the targeting of ten-eleven translocation 3 (TET3), as well as via multiple negative regulators of the Wnt/ $\beta$ -catenin pathway including glycogen synthase kinase-3 beta (GSK3 $\beta$ ) and casein kinase 1a (CK1 $\alpha$ ); this miRNA is therefore linked to the consequent increase in the CSC subpopulations in OS that have been observed both in vitro and in vivo. In addition, treatment with a miR-135b antagomiRNA (antagomiR) suppressed the metastasis of OS cells to the lung, as well as CSC-induced tumorigenesis and recurrence in animal models. Our results suggest that miR-135b plays an important role in the maintenance of stem cell-like properties of a subset of OS cells, and that this miRNA is a potential therapeutic target in cases of OS lung metastasis and recurrence.

## RESULTS

### miR-135b Is Aberrantly Upregulated in OS and Is Correlated with Metastasis

First, we quantified the expression level of miR-135b in OS tumors and cell lines. As shown in Figures 1A and 1B, the expression of miR-135b was significantly increased in primary tumors of OS patients and in OS cell lines compared with adjacent non-tumor tissues and human fetal osteoblastic cells (hFOBs), respectively. Interestingly, our data show that the expression of miR-135b was significantly increased in tissues from recurrent OS that metastasized to the lung compared with the corresponding primary tumors (Figure 1C). Consistent with these clinical data, the expression of miR-135b was also significantly increased in highly metastatic OS cell lines (LM-5 and M132) compared with their less metastatic parental cell lines (Saos-2 and HuO9) (Figure 1D). Collectively, our data clearly indicate that miR-135b is markedly upregulated in OS and might play a role in OS metastasis and recurrence.

### Overexpression of miR-135b Stimulates OS Metastasis and Recurrence

To address whether miR-135b plays a role in OS metastasis and recurrence, we first used MG63, Saos-2, and HuO9 cells to establish stable miR-135b-overexpressing OS cell lines. In addition, we stably silenced miR-135b in the MNNS/HOS and LM5 cell lines. As shown

in Figures S1A and S1B, the miR-135b levels were markedly increased in the miR-135b-overexpressing OS cells, whereas decreased levels were observed in the OS cells with stably silenced miR-135b compared with the vector control. In addition, our data show that the stable overexpression of miR-135b significantly promoted MG63 and Saos-2 cell migration and invasion in vitro (Figure 1E). More importantly, our in vivo experiment shows that the stable overexpression of miR-135b induced the metastasis of Saos-2 cells to the lungs in nude mice, whereas the vector control Saos-2 cells did not induce lung metastasis (Figure 1F). Together, these findings suggest that miR-135b has a strong role in the promotion of lung metastasis of OS.

Next, to determine whether the high expression of miR-135b was associated with OS recurrence, we inoculated the mice with Saos-2-vector or Saos-2-miR-135b-overexpressing cells. When the mean tumor volume reached  $70 \pm 16 \text{ mm}^3$ , the mice began to receive cisplatin (CDDP) treatment, which lasted for 12 days. As shown in Figure 1G, after a transient reduction in mass volume, tumors that expressed a higher level of miR-135b continued to grow, whereas tumor xenografts of vector control cells failed to regrow in a 30-day period. These data suggest that miR-135b essentially contributes to OS recurrence in vivo.

### Overexpression of miR-135b Promotes a Stem Cell-like Phenotype in OS

Because some studies have revealed that CSCs are involved in tumor metastasis and relapse,<sup>14</sup> we speculated that miR-135b might be involved in the regulation of stemness of OS cells. To address this hypothesis, we first used an antibody against the CSC marker protein CD133 and an antibody against acetaldehyde dehydrogenase 1 (ALDH1) to separate CSCs and non-CSCs from OS cells; then the miR-135b expression was quantified. The results show that miR-135b was more highly expressed in CD133- and ALDH1-positive Saos-2 and HuO9 cells compared with negative cells (Figure 2A). In turn, the overexpression of miR-135b dramatically increased the percentage of CD133- and ALDH1-positive Saos-2 and HuO9 cell populations compared with their corresponding vector controls (Figures 2B and 2C). Consistent with these findings, the expression of CSC marker proteins, including Nanog, BMI1, and Oct4, was significantly increased in Saos-2 and HuO9 cells that were stably transduced with miR-135b compared with the vector control cells (Figure 2D). Furthermore, a sphere formation assay shows that Saos-2 and HuO9 cells transduced with miR-135b formed more spheres than the vector control cells (Figure 2E). These findings suggest that miR-135b strongly promotes the stem-like characteristics of OS cells.

### Overexpression of miR-135b Activates Notch and Wnt/ $\beta$ -Catenin Signaling to Promote CSC Traits in OS

To investigate the mechanism of miR-135b in the regulation of OS cell stemness, we confirmed the effects of miR-135b in Notch and Wnt/ $\beta$ -catenin signaling. The Notch and Wnt/ $\beta$ -catenin signaling pathways are hyperactivated in CSCs and contribute to

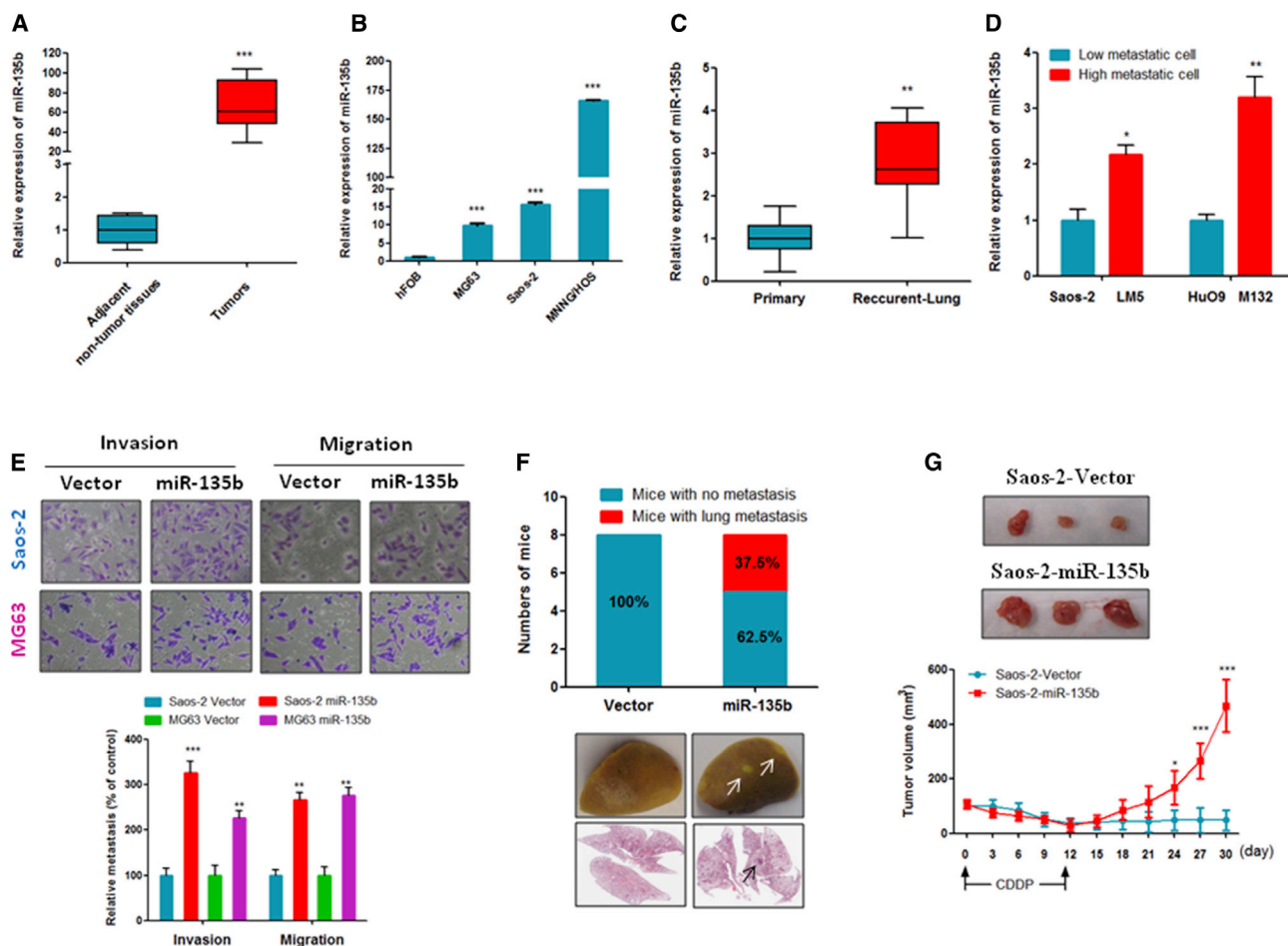


**Figure 1. The Expression of miR-135b Was Increased in OS Specimens and OS Cell Lines, and Increased miR-135b Enhances Lung Metastasis and Recurrence of OS**

miR-135b expression was measured by qRT-PCR. Assays were performed in triplicate, and the results are presented as the mean  $\pm$  SEM. (A) miR-135b was significantly increased in OS tissues compared with their adjacent non-tumor tissues. OS tissues and their adjacent non-tumor tissues were collected from 30 patients with OS ( $n = 30$ ). (B) miR-135b was overexpressed in OS cell lines compared with human fetal osteoblastic (hFOB) cells. (C) miR-135b expression was significantly increased in recurrent pulmonary metastatic OS specimens compared with their corresponding primary OS tumors ( $n = 10$ ). (D) miR-135b was overexpressed in highly metastatic OS cell lines compared with their less metastatic parental cell lines. (E) Overexpression of miR-135b stimulated the invasiveness and migration of Saos-2 and MG63 cells. (F) Overexpression of miR-135b increased the ability of Saos-2 cells to metastasize to the lungs in vivo ( $n = 8$  mice/group). Representative gross image of a lung (middle) and H&E-stained lung sections (bottom) from animals intravenously injected with Saos-2 cells that stably expressed miR-135b. Arrows indicate visible lesion. (G) miR-135b-transduced Saos-2 cells and vector control cells were injected subcutaneously into nude mice ( $n = 6$  mice/group). When the mean tumor volume reached  $70 \pm 16 \text{ mm}^3$ , the mice were intraperitoneally injected with CDDP every 3 days for a total of four rounds. The tumor volume was measured every 3 days. \* $p < 0.05$ ; \*\* $p < 0.01$ ; \*\*\* $p < 0.001$ .

the maintenance of cell stemness in several cancer types.<sup>29,30</sup> Similar to other cancers, the expression of  $\beta$ -catenin and Notch1, as well as the Notch1 downstream protein HES1, were significantly increased in CD133- and ALDH1-positive OS cells compared with CD133- and ALDH1-negative OS cells (Figure 3A). Further, our data show that the expression of the downstream Notch signaling protein HES1 and the activity of the luciferase reporter driven by Wnt/ $\beta$ -catenin signals were significantly increased in miR-135b stably transduced OS cells compared with the vector control cells (Figures 3B and 3C). In addition, subcellular fractionation analysis showed that the overexpression of miR-135b increased the nuclear accumulation

of  $\beta$ -catenin in Saos-2 and HuO9 cells (Figure 3D). Furthermore, we confirmed such increased expression of HES1 and  $\beta$ -catenin in miR-135b-overexpressing Saos-2 cells by immunofluorescence (Figure 3E). Consistent with the in vitro data, the expression of HES1 and  $\beta$ -catenin was also increased in xenograft tumor tissues that formed from miR-135b stably transduced Saos-2 cells compared with the control (Figure 3F). In contrast, the expression of HES1 and  $\beta$ -catenin activity were suppressed in miR-135b stably silenced MNNG/HOS cells compared with the vector control cells (Figure S2), which suggests that miR-135b positively regulates Notch and Wnt/ $\beta$ -catenin signaling in OS cells.

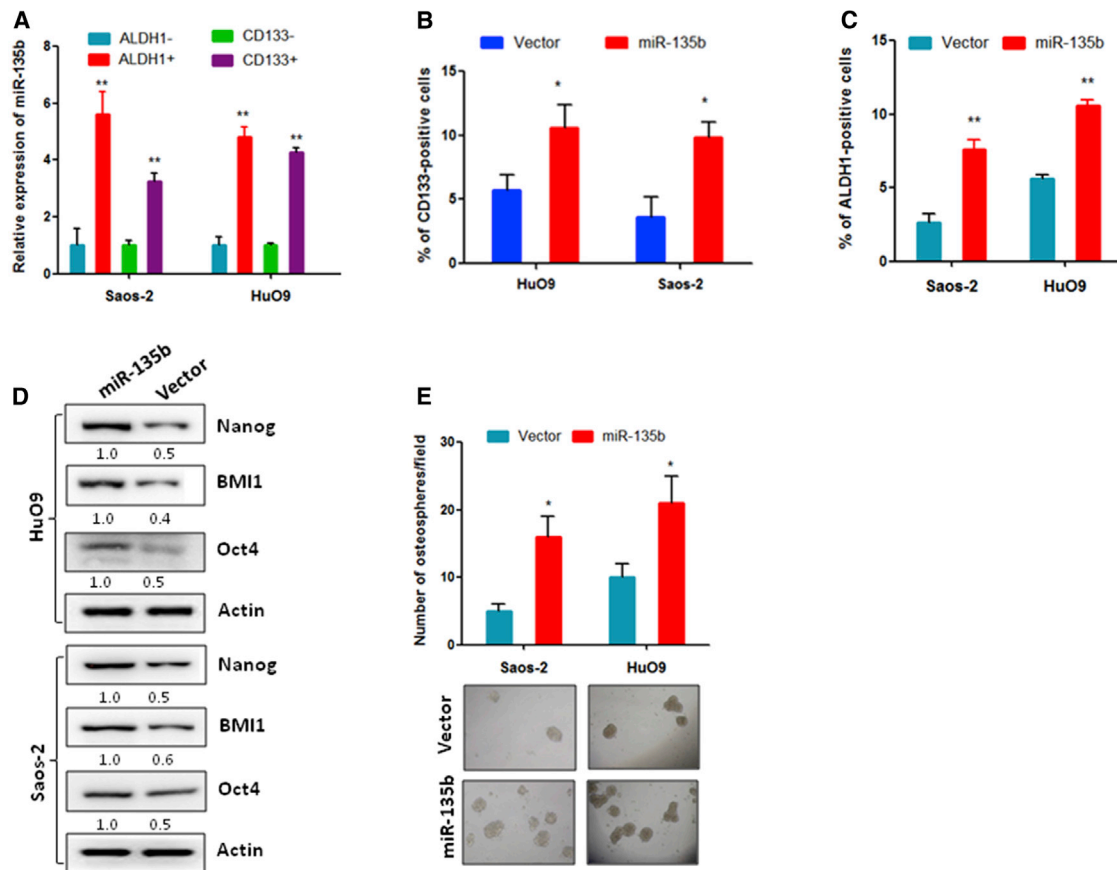


**Figure 2. miR-135b Promotes Stem Cell-like Properties in OS Cells**

(A) miR-135b was overexpressed in CD133-positive and ALDH1-positive OS cells compared with CD133-negative and ALDH1-negative OS cells. (B) CD133-positive populations were increased in HuO9 and Saos-2 cells that stably expressed miR-135b compared with their corresponding vector control cells. (C) ALDH1-positive populations were increased in HuO9 and Saos-2 cells that stably expressed miR-135b compared with their corresponding vector control cells. (D) The expression of cancer stem cell marker proteins was dramatically increased in cells that stably expressed miR-135b compared with the control. (E) Overexpression of miR-135b stimulated osteosphere formation in the indicated cell lines. \* $p < 0.05$ ; \*\* $p < 0.01$ .

Next, to investigate whether  $\beta$ -catenin affects the miR-135b-induced activation of the Notch pathway, we knocked down  $\beta$ -catenin expression in miR-135b stably transduced OS cells by transfection of short hairpin RNA (shRNA) (Figure S3A), because studies have shown that  $\beta$ -catenin can activate Notch signaling.<sup>28,31</sup> Our results show that the silencing of  $\beta$ -catenin partially suppressed the expression of the miR-135b-induced Notch signaling target gene HES1, but the suppression was not complete (Figure 3G), which suggests that miR-135b activates Notch signaling via both  $\beta$ -catenin-dependent and -independent mechanisms in OS cells.

Further, we investigated whether activated Notch and Wnt/ $\beta$ -catenin signaling affects the biological function of miR-135b in OS cells. As shown in Figures 3B–3E, the silencing of Notch1 or  $\beta$ -catenin partially inhibited the miR-135b-induced stem cell-like phenotype and metastasis in OS cells. Importantly, our data show that the knock-down of both Notch1 and  $\beta$ -catenin more completely inhibited stemness and metastasis in miR-135b-overexpressing OS cells. In addition,

our animal experiments show that treatment of Notch and Wnt/ $\beta$ -catenin signaling inhibitors significantly inhibited miR-135b over-expressing Saos-2 cell-induced lung metastasis and recurrence (Figures 3F and 3G). Taken together, these data suggest that miR-135b stimulates the OS lung metastasis, recurrence, and stemness of OS cells through the activation of both the Notch and the Wnt signaling pathways in OS cells.

#### miR-135b Activates the Notch and Wnt/ $\beta$ -Catenin Pathways by the Direct Targeting of the Negative Regulators of Wnt/ $\beta$ -Catenin and Notch Signaling in OS Cells

To investigate the mechanism that underlies the effect of miR-135b on the activation of Notch and Wnt/ $\beta$ -catenin signaling in OS cells, we screened miR-135b target genes using the computational algorithms TargetScan v6.2, miRanda and miRDB. We identified four negative regulators of the Wnt/ $\beta$ -catenin pathway, namely, GSK3 $\beta$ , adenomatous polyposis coli (APC), CK1 $\alpha$ , and  $\beta$ -transducin repeats-containing proteins ( $\beta$ -TrCPs), as miR-135b putative target genes that could

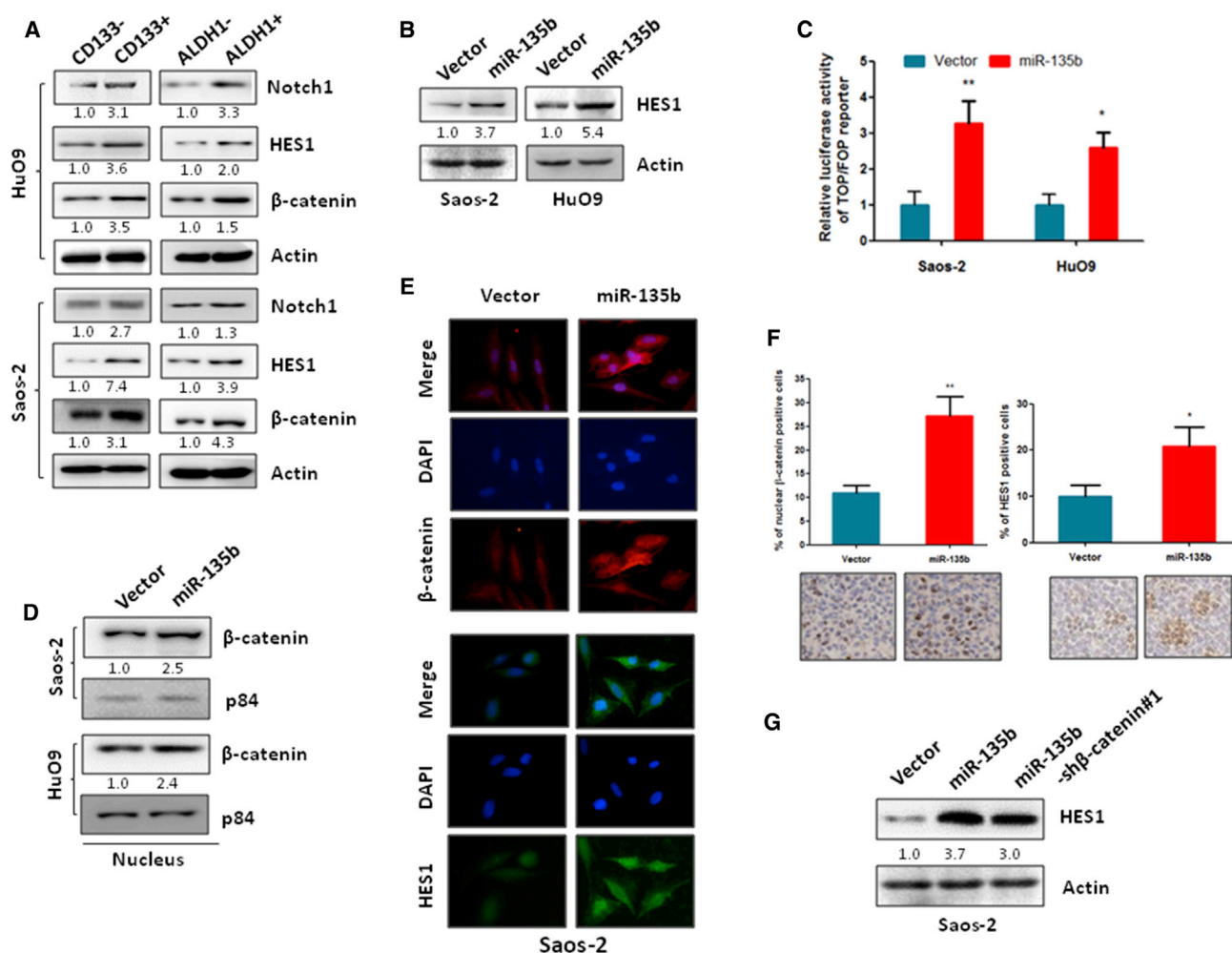


**Figure 3. miR-135b Activates the Notch1 and Wnt/β-Catenin Pathways**

(A) The expression of Notch1, HES1, and β-catenin was significantly increased in CD133- and ALDH1-positive cells compared with CD133- and ALDH1-negative cells, respectively. (B) The expression of HES1 was increased in OS cells that stably expressed miR-135b compared with their corresponding vector control cells. (C) β-Catenin activity was increased in miR-135b-transduced OS cells compared with their corresponding vector control cells. The indicated cells were transfected with TOP or FOP reporter and Renilla pRL-TK plasmid and were subjected to a dual-luciferase assay 48 hr after transfection. (D) The level of β-catenin in the nucleus was increased in cells that stably expressed miR-135b compared with the vector control cells. Nuclear fractions were extracted from the indicated cells, and the indicated proteins were analyzed by western blot. p84 was used as a loading control. (E) The expression of β-catenin and HES1 was assessed by immunofluorescence staining of Saos-2 cells. (F) Immunohistochemistry analysis of HES1 and β-catenin in xenograft tumors that induced by miR-135b transduced Saos-2 cell and vector control cells. (G) The silencing of β-catenin partially inhibited the miR-135b-induced HES1 expression in Saos-2 cells. Saos-2 cells were transfected with the indicated plasmid, and the expression of the proteins shown was measured by western blot 72 hr after transfection. \* $p < 0.05$ ; \*\* $p < 0.01$ .

potentially be suppressed by miR-135b (Figure 4A). Additionally, we selected TET3 as a putative target gene of miR-135b (Figure 4A). This is because TET3 increases the expression of miR-200 family members via the demethylation of the miR-200 promoter<sup>32</sup> and because miR-200 can negatively regulate Notch signaling.<sup>33</sup> To investigate the regulation of miR-135b on the expression of putative target genes in OS cells, we measured the expression of target genes in miR-135b stably transduced and stably silenced OS cells, as well as the vector control cells. As shown in Figures 4B and 4C, the expression levels of TET3, GSK3β, β-TrCP, CK1α, and APC were significantly decreased in

miR-135b-overexpressing OS cells compared with vector control cells at both the mRNA and the protein levels. In contrast, the expression levels of TET3, GSK3β, β-TrCP, CK1α, and APC were significantly increased in miR-135b-silenced MNNG/HOS cells at both the mRNA and the protein levels (Figures 4A and 4B), which suggests that miR-135b negatively regulates the expression of TET3, GSK3β, β-TrCP, CK1α, and APC in OS cells.

Next, we confirmed the direct binding of miR-135b to its target genes by RNA immunoprecipitation (RIP) and luciferase reporter assays.

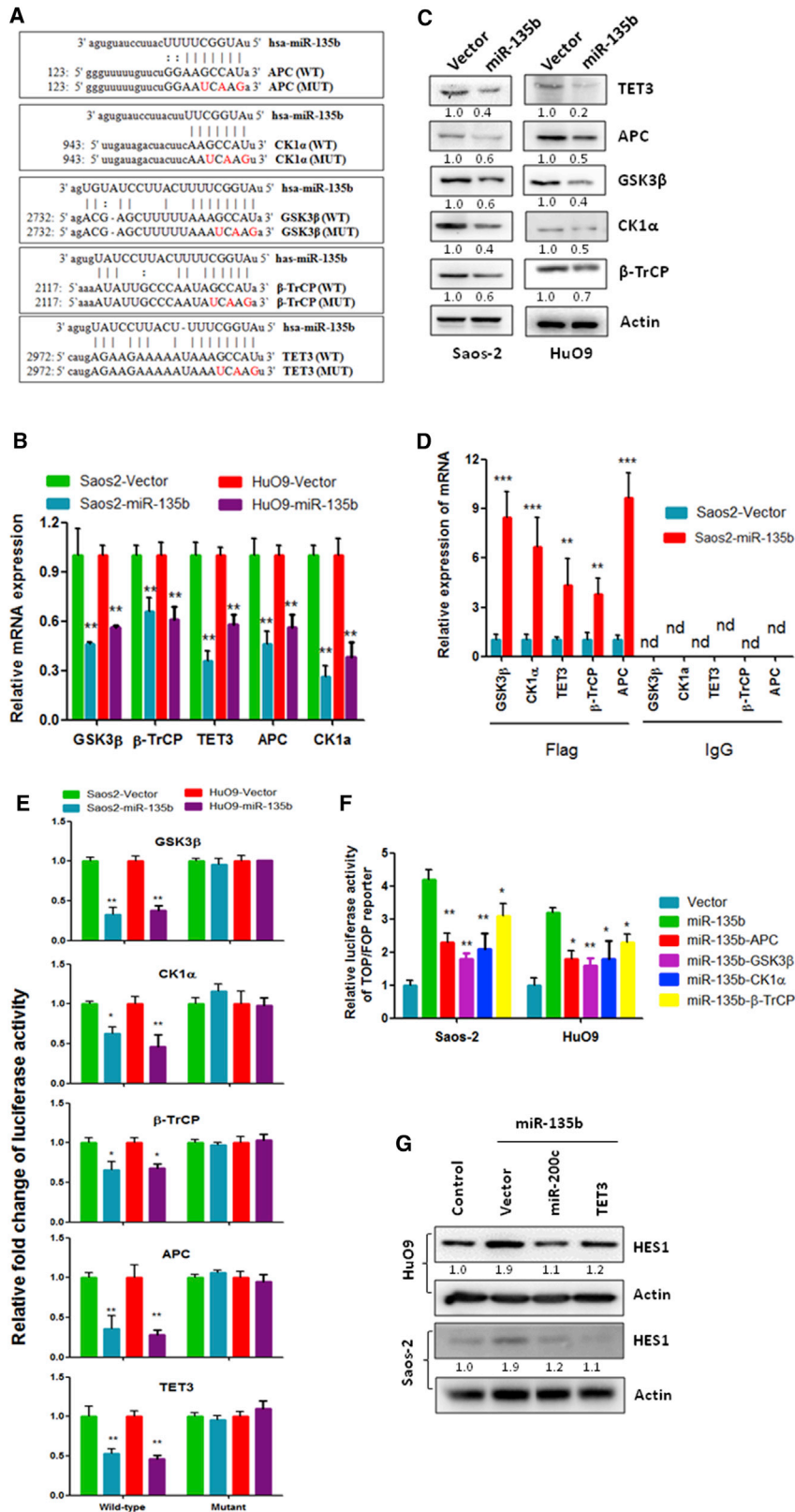


**Figure 4. miR-135b Directly Targets TET3 and Multiple Negative Regulators of the Wnt/ $\beta$ -Catenin Pathway**  
 (A) Predicted binding sites of miR-135b in the 3' UTR of the indicated genes. (B and C) qRT-PCR (B) and western blot analysis (C) of the expression of the indicated genes in the cells shown. (D) RIP analysis revealed that mRNAs of the indicated genes were recruited to miRNA-protein (miRNP) complexes following immunoprecipitation with flag (flag-Ago2). IgG immunoprecipitation was used as a negative control. (E) Activity of the luciferase gene was linked to the 3' UTRs of the indicated genes. The luciferase reporter plasmids (wild or mutated 3' UTR sequences of the indicated genes) were transfected into the indicated cells, and the luciferase activity was measured 48 hr after transfection. (F) The indicated cells were transfected with the indicated genes and a TOP or FOP reporter and were then subjected to a dual-luciferase assay 48 hr after transfection. (G) The indicated cells were transfected with the indicated genes and were subjected to western blot analysis 72 hr after transfection. \* $p < 0.05$ ; \*\* $p < 0.01$ ; \*\*\* $p < 0.001$ . nd, not detected.

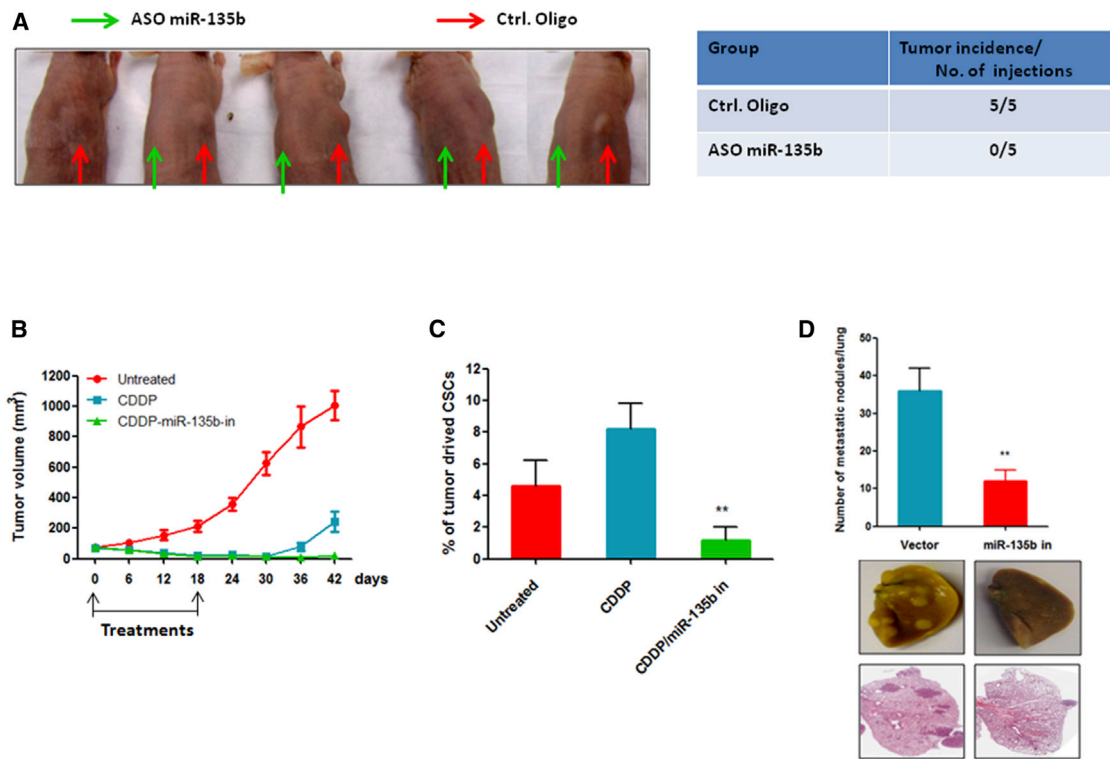


**Figure 5. Inhibition of miR-135b Inhibits OS Metastasis and CSC-Induced Tumorigenesis and Recurrence**

(A) Inhibition of miR-135b suppressed CD133<sup>high</sup> Saos-2 cell-induced tumor formation in nude mice. CD133<sup>high</sup> Saos-2 cells transfected with antisense nucleotides of miR-135b (ASO miR-135b) or negative control nucleotides (Ctrl. Oligo). After 12 hr of transfection, cells were subcutaneously injected into nude mice (n = 5). (B) Combination treatment of CDDP and antagonism of miR-135b inhibited OS recurrence. CD133<sup>high</sup> Saos-2 cells were subcutaneously injected into nude mice (n = 6 mice/group). When the mean tumor volume reached  $70 \pm 21$  mm<sup>3</sup>, the mice were intraperitoneally injected with CDDP and antagonism of miR-135b (miR-135b in) or with the antagonism of negative control every 3 days for six total rounds. The tumor volume was measured every 3 days. (C) The proportion of CD133-positive cells derived from xenograft tumors is shown. Tumors were collected from xenograft mice (n = 3/group) 12 days after the start of treatment. (D) Inhibition of miR-135b significantly suppressed the ability of LM5 cells to metastasize to the lungs in vivo (n = 6/group). \*\*p < 0.01.

RIP analysis by anti-flag (Ago-flag) showed that the expression of target genes was increased in miR-135b-transduced OS cells at the mRNA level (Figure 4D), whereas the expression of target genes was decreased in miR-135b-silenced OS cells compared with the vector control cells (Figure 4C). This suggests that miR-135b might be specifically recruited by putative target genes to the miRNA protein (miRNP) complex. Moreover, the luciferase reporter assay shows that luciferase activity of the plasmid containing the wild-type 3' UTR of the putative target genes was significantly reduced in miR-135b-overexpressing OS cells; in contrast, no effects were observed when mutations were introduced into the putative target site (Figure 4E), which suggests that miR-135b directly interacts with the 3' UTR of these target genes in OS cells.

Further, we investigated whether these target genes directly contribute to the miR-135b-induced activation of Notch and Wnt/ $\beta$ -catenin signaling. To address this question, we separately transfected the target genes of miR-135b into miR-135b-overexpressing Saos-2 and HuO9 cells (Figure 5A) and then measured Wnt/ $\beta$ -catenin pathway activity and the expression of Notch signaling-related

proteins. As shown in Figure 4F, the separate transfection of CK1 $\alpha$ ,  $\beta$ -TrCP, APC, and GSK3 $\beta$  partially inhibited the miR-135b-induced activation of Wnt/ $\beta$ -catenin signaling in miR-135b-overexpressing OS cells. These findings suggest that miR-135b contributes to the activation of the Wnt/ $\beta$ -catenin pathway via the targeting of CK1 $\alpha$ ,  $\beta$ -TrCP, APC, and GSK3 $\beta$  in OS cells. Furthermore, we examined the effects of the TET3/miR-200c axis on the miR-135b-induced activation of Notch signaling. Our data show that the overexpression of TET3 or miR-200c (Figures 5B and 5C) significantly inhibited the miR-135b-induced activation of Notch signaling (Figure 4G), which suggests that the TET3/miR-200 axis is one of the major players responsible for the activation of Notch signaling by miR-135b in OS cells.

#### **Inhibition of miR-135b Effectively Suppresses Lung Metastasis, CSC-Induced Tumorigenesis, and Recurrence in OS**

Our observations that the overexpression of miR-135b promotes metastasis of OS to the lungs, recurrence, and CSC traits prompted us to investigate whether miR-135b inhibition could suppress lung metastasis and CSC-induced tumorigenesis and recurrence. To

address this possibility, we sorted CSCs (CD133-high-expressing cells) from Saos-2 cells and transfected them with the antisense of miR-135b or with control oligonucleotides. The cells were then subcutaneously inoculated into nude mice (right side of the back: CD133<sup>high</sup> cells transfected with control oligonucleotide; left side of the back: CD133<sup>high</sup> cells transfected with the antisense of miR-135b). As shown in Figure 5A, transfection of the cells with control oligonucleotides did not affect tumor formation by CSCs. However, the inhibition of miR-135b completely inhibited tumor formation by CSCs in nude mice, which suggests that the inhibition of miR-135b can effectively suppress CSC-induced tumorigenesis in OS.

Next, we investigated whether the inhibition of miR-135b affects OS relapse in vivo. When the mean tumor volume reached  $70 \pm 21 \text{ mm}^3$ , the mice that were inoculated with CD133<sup>high</sup> Saos-2 cells began to receive intraperitoneal injections of CDDP with antagomiR-135b or control antagomiR; this treatment lasted for 18 days. Our results show that a single treatment with CDDP caused tumor regression, but that the relapse of the disease occurred 12 days after the treatment ended. By contrast, combined treatment consisting of CDDP and miR-13b inhibition could effectively prevent tumor relapse (Figure 5B). To determine whether the combination therapy of CDDP and miR-135b inhibition could reduce the proportion of CSCs in vivo, we examined the populations of CSCs recovered from xenograft tumors. After four cycles of treatment, the proportions of CSCs were significantly decreased in xenograft tumors from the combined treatment group of CDDP and miR-135b inhibition compared with tumors from the CDDP single-treatment group and the control group (Figure 5C). Taken together, these data suggest that the inhibition of miR-135b is essential for the inhibition of CSC-induced disease relapse in OS.

Further, we evaluated the effect of the silencing of miR-135b on the metastasis of OS cells to the lungs. We used the highly metastatic OS cell line LM5 to establish a miR-135b-silenced cell line (Figure 1B). We then administered these cells to nude mice by tail vein injection. The results show that the inhibition of miR-135b dramatically suppressed the formation of LM5 cell-induced metastatic lesions in the lungs of mice compared with the vector control cells (Figure 5D), which suggests that the inhibition of miR-135b can inhibit the metastasis of OS cells to the lungs.

#### Clinical Relevance of miR-135b and Its Targets in Human OS Specimens

To further understand the potential biological significance of deregulated miR-135b expression in the progression of OS, we evaluated the correlation between miR-135b expression and survival in 112 patients with OS. Our data show that patients whose tumors highly expressed miR-135b had lower overall survival and recurrence-free survival rates than those whose tumors expressed low levels of miR-135b (Figure 6A). Moreover, the univariate and multivariate analyses show that the miR-135b expression level was a risk factor for survival outcome in patients with OS (Table S3). Next, we examined the potential relationship between miR-135b and its target genes in OS clinical samples. As shown in Figure 6B, significant inverse correlations between

miR-135b and TET3, CK1 $\alpha$ , and GSK3 $\beta$  were observed, whereas the expression of miR-135b was positively correlated with Notch1 and  $\beta$ -catenin expression in OS specimens. In addition, the data show that high expression of Notch1 and/or  $\beta$ -catenin was strongly associated with poor clinical outcomes of OS patients (Figure 6C). These data suggest that miR-135b, Notch1, and  $\beta$ -catenin expression may be a useful prognostic signature of OS. However, we did not observe any correlation between the expression of miR-135b and APC or  $\beta$ -TrCP in clinical samples of OS (Figure 6C), which suggests that APC and  $\beta$ -TrCP are not major target genes of miR-135b in OS. Overall, our results demonstrate that miR-135b activates Notch and Wnt/ $\beta$ -catenin signaling by targeting TET3, CK1 $\alpha$ , and GSK3 $\beta$ , enhances stem cell-like traits, and leads to tumor recurrence and poor prognosis in patients with OS (Figure 6D).

#### DISCUSSION

Aberrantly expressed miR-135b and its function in OS have been previously reported, but the results are inconsistent.<sup>34,35</sup> Here, we report that miR-135b was significantly increased in OS tissue and OS cells, and has an oncogenic function in OS. Such results are consistent with most OS studies that have been reported by other research groups.<sup>25,36</sup> Furthermore, overexpressed miR-135b and its oncogenic function were identified previously in a variety of tumors including colon,<sup>34</sup> breast,<sup>35</sup> prostate,<sup>37</sup> and lung<sup>38</sup> cancers, which suggests that miR-135b plays a general role in different types of cancers. However, in previous studies, the tumor promotion function of miR-135b in OS mainly focused on cell proliferation and invasion in vitro. In this report, for the first time, we used in vitro and in vivo experiments to provide compelling biological and clinical evidence that miR-135b can significantly promote cancer cell stemness, lung metastasis, and tumor recurrence in OS. Notably, our clinical data show that the upregulated expression of miR-135b was closely associated with poor clinical outcomes, and the miR-135b expression level was a risk factor for survival outcome in patients with OS, which strongly suggests that miR-135b acts as an onco-miRNA in OS because it significantly promotes OS progression.

In this study, we also clarified the tumor promotion mechanism of miR-135b in OS. CSCs play a major role in tumor progression, including metastasis and recurrence, after traditional treatment.<sup>17</sup> Evidence indicates that constitutively activated Wnt/ $\beta$ -catenin and Notch signaling is critical for the development and maintenance of CSCs.<sup>39–41</sup> GSK3 $\beta$ , APC, and  $\beta$ -TrCP are negative regulators of Wnt/ $\beta$ -catenin signaling and have been identified as targets of miR-135b in glioblastoma,<sup>41</sup> colon cancer,<sup>34</sup> and lung cancer,<sup>38</sup> respectively. These results are consistent with our findings. Our in vitro data also show that miR-135b activates Wnt/ $\beta$ -catenin signaling via direct targeting of GSK3 $\beta$ , APC, and  $\beta$ -TrCP in OS cells. In addition, we identified CK1 $\alpha$  as a new target gene of miR-135b in OS cells that is another negative regulator of Wnt/ $\beta$ -catenin signaling. Importantly, ectopic expression of these genes can inhibit cancer-promoting effects of miR-135b in OS cells. However, unlike in our in vitro work, we observed a correlation solely between miR-135b and GSK3 $\beta$  or CK1 $\alpha$  in OS patient specimens, but we did not observe a correlation between miR-135b and APC or  $\beta$ -TrCP. This suggests that GSK3 $\beta$

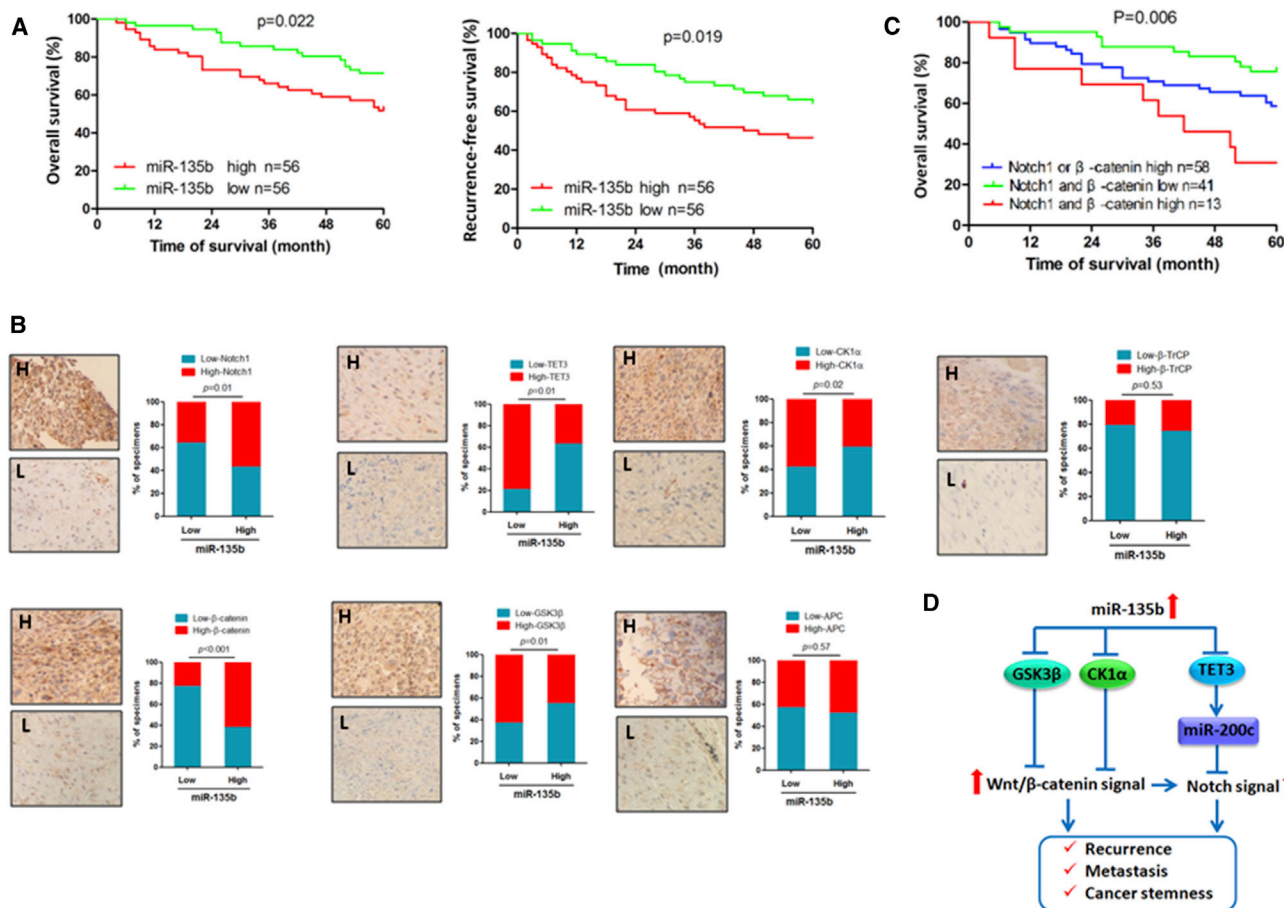


**Figure 6. Clinical Relevance of miR-135b Expression and the Expression of Its Target Genes in Human OS Tissues**

(A) The correlation between the miR-135b level and the 5-year overall survival and the recurrence-free survival of 112 patients with OS was analyzed using the Kaplan-Meier method. (B) The correlation between miR-135b and its target genes in OS specimens was determined by qRT-PCR and immunohistochemical analysis, which were used to measure the expression of miR-135b and the expression of its target genes, respectively. (C) The correlation between the Notch1 and  $\beta$ -catenin levels with the 5-year overall survival rate in 112 patients with OS was analyzed using the Kaplan-Meier method. (D) Illustration of Notch and Wnt/ $\beta$ -catenin activation by miR-135b via the suppression of multiple target genes.

and CK1 $\alpha$  are the major players responsible for miR135b-induced activation of Wnt/ $\beta$ -catenin signaling in OS. Furthermore, we identified that miR-135b activates Notch signaling via both Wnt/ $\beta$ -catenin pathway-dependent and -independent mechanisms in OS cells. Our data show that inhibition of  $\beta$ -catenin cannot completely suppress the miR-135b-induced activation of the Notch pathway in OS cells, which suggests the existence of a  $\beta$ -catenin-independent mechanism for the activation of Notch signaling. Here, we identified TET3 as a target gene of miR-135b in OS cells. According to previous reports, TET3 functions as tumor suppressor to inhibit cancer cell stemness and tumor metastasis.<sup>32,42</sup> Moreover, the anticancer effects of TET3 are partially through positive regulation on members of the miR-200 family,<sup>32,42</sup> which have been identified as negative regulators of Notch signaling.<sup>33</sup> Consistent with these reports, our data also show that TET3 can increase miR-200c expression and that overexpression of TET3 or miR-200c can inhibit miR-135b-induced Notch signaling activation and tumor promotion. Notably, clinical data show that

TET3 expression level is negatively correlated with miR-135b level in OS specimens. These findings suggest that miR-135b activates Notch signaling partially because of the inhibition of the TET3/miR-200c axis via the direct targeting of TET3 in OS cells. Taken together, these findings suggest that aberrantly upregulated expression of miR-135b promotes OS progression through significantly activating and sustaining both Wnt/ $\beta$ -catenin and Notch signaling simultaneously in OS via the suppression of multiple negative regulators of these signaling networks. This also provides a new molecular mechanism by which miR-135b mediates stem cell-like properties of OS cells.

In the current study, we also evaluated the potential of miR-135b to serve as a therapeutic target in OS. The significant contributions of Wnt/ $\beta$ -catenin and Notch signaling to CSCs have been well defined in a wide variety of cancer types, which suggests that the targeting of these two pathways is a promising therapeutic strategy to address tumor chemoresistance, metastasis, and recurrence.<sup>43,44</sup> In fact, the

$\beta$ -catenin inhibitor ICG-001<sup>45</sup> and the Notch inhibitor BMS-906024 (NCT01292655) are currently being tested in phase I clinical trials. However, Wnt/ $\beta$ -catenin and Notch signaling were found to be simultaneously activated in CSCs of OS, and their oncogenic functions were partly from different pathways.<sup>44,46</sup> More importantly, research has shown that the inhibition of Notch can activate Wnt/ $\beta$ -catenin signaling,<sup>21</sup> which indicates that a combination treatment that consists of  $\beta$ -catenin and Notch inhibitors is more effective for cancer therapy. In fact, studies have shown that combined treatment consisting of  $\beta$ -catenin and Notch inhibitors significantly enhances the anticancer effects observed with individual therapies.<sup>47,48</sup> Our current study shows that antagonizing miR-135b caused the inactivation of both Wnt/ $\beta$ -catenin and Notch signaling simultaneously and exerted dramatic inhibitory effects on metastasis, CSC-induced tumorigenesis, and the recurrence of OS in xenografts models. This suggests that miR-135b may be a novel therapeutic target, and that inhibition of miR-135b can suppress both Wnt/ $\beta$ -catenin and Notch signaling to suppress lung metastasis and CSC-induced tumorigenesis and recurrence in OS.

In summary, here we identified novel roles for miR-135b in OS. Aberrantly upregulated expression of miR-135b contributes to OS cell stemness, metastasis, and recurrence through the activation of Wnt/ $\beta$ -catenin and Notch signaling via the direct targeting of multiple negative regulators of these networks. The inhibition of miR-135b suppressed OS metastasis, CSC-induced tumorigenesis, and recurrence. Notably, in the current study, miR-135b demonstrated positive correlations with both poor prognosis and recurrence in patients with OS. These findings suggest that miR-135b is a useful prognostic indicator and a potential candidate for the treatment of OS metastasis and the prevention of OS recurrence.

## MATERIALS AND METHODS

### Cell Culture

hFOB, Saos-2, MG63, and MNNG/HOS cells were purchased from the American Type Culture Collection. LM5, HuO9, and LM132 cells were obtained from Moffitt Cancer Center. HuO9 and HuO9-M132 (M132) cells were maintained in RPMI 1640 medium; hFOB, Saos-2, and Saos-2-LM5 cells (LM5) were maintained in DMEM/Ham F12 (1:1); MG-63 cells were maintained in DMEM; and MNNG/HOS cells were maintained in Eagle's Minimum Essential Medium at 37°C in an atmosphere of 95% air and 5% CO<sub>2</sub>. All cell cultures were supplemented with 10% fetal bovine serum (Gibco), 100 U/mL penicillin, and 100  $\mu$ g/mL streptomycin (Sigma).

### Plasmids and Transfection

The 3' UTRs of TET3, GSK3 $\beta$ , CK1 $\alpha$ , APC, and  $\beta$ -TrCP were amplified from human genomic DNA and cloned downstream of the luciferase gene in an miRNA Expression Reporter Vector (Promega). The expression plasmids of miR-135b, miR-135b antisense, cMyc-APC, flag-TET3, cMyc-GSK3 $\beta$ , and cMyc-CK1 $\alpha$  were from GeneCopoeia. Flag- $\beta$ -TrCP was a gift from Peter Howley (Addgene plasmid 10865).<sup>49</sup> Flag-Ago2 construct was kindly provided by Dr. Cheng (Moffitt Cancer Center). Top and Fop reporter plasmids

were purchased from Millipore. All transfections were performed using Lipofectamine 2000 reagent (Invitrogen).

### Tissue Samples and Animal Study

Human specimens were obtained by biopsy from 112 OS patients with no metastasis at diagnosis under a protocol approved by the review boards of the General Hospital of Chinese People's Liberation Army. OS tissues were obtained at biopsy for diagnosis, and their non-tumor tissues and pulmonary metastatic samples were collected during surgery. All patients received the same treatment, and the patient characteristics at the time of the original diagnosis are summarized in Table S1.

Animal care was in accordance with institutional guidelines, and all animal experiments were approved by the Animal Care Committee. Six-week-old female athymic nu/nu mice were used for all animal experiments. For the lung metastasis experiments, the lateral tail veins of mice were injected with  $4 \times 10^5$  of the indicated cells in 150  $\mu$ L of serum-free medium. Mice were sacrificed 4 weeks after injection of the cells, and the metastatic nodules on the lung surface were counted. For tumor relapse experiments,  $5 \times 10^6$  miR-135b stably transduced Saos-2 cells, vector control Saos-2 cells, or  $1 \times 10^5$  CD133<sup>high</sup> Saos-2 cells in serum-free medium were subcutaneously injected into mice. When the tumors reached a volume of  $\sim 70$  mm<sup>3</sup>, the mice were treated with CDDP (5 mg/kg body weight) or antagomiR-135b (10  $\mu$ M in 100  $\mu$ L of PBS) by intraperitoneal injection every 3 days for the indicated number of days. For the CSC tumor formation experiment, CD133<sup>high</sup> Saos-2 cells were isolated and transfected with the indicated oligonucleotides (Life Technologies). Then, 12 hr after transfection,  $1 \times 10^4$  cells in serum-free medium were subcutaneously injected into mice.

### Transwell and Osteosphere Formation Assay

For the Transwell assay,  $1 \times 10^5$  cells in serum-free growth medium were seeded into the upper wells of BD migration or invasion chambers (12-well plate). The lower wells contained the same medium supplemented with 10% serum. After 24 hr, the cells that had migrated to the lower side of the chamber were fixed, dyed, and counted as previously described.<sup>14</sup> For the osteosphere formation assay, 1,000 cells were seeded in six-well ultra-low cluster plates (Corning) and cultured for 8 days. The cells were cultured in serum-free DMEM/F12 medium with 1% methylcellulose (Sigma), 20 nM progesterone (Sigma), 100  $\mu$ M putrescine (Sigma), 1% insulin-transferrin-selenium A supplement (GIBCO), 10 ng/mL basic fibroblast growth factor (bFGF; Peprotech EC), and 10 ng/mL human recombinant epidermal growth factor (Sigma).<sup>11</sup>

### Flow Cytometric Analysis

CSCs were detected using flow cytometric analysis. ALDH1-positive cells were detected or isolated using the ALDEFLUOR fluorescent reagent system (STEMCELL Technologies, Vancouver, BC, Canada) according to the manufacturer's instructions. CD133-positive cells were detected or isolated using a CD133 antibody (Abcam) as described by Tirino et al.<sup>12</sup>

### Luciferase Reporter Assay

The indicated cells were seeded in 24-well plates and allowed to settle for 24 hr. The cells were transfected with the indicated plasmid and with the pPL-TK Renilla plasmid using Lipofectamine 2000 reagent. Then, 48 hr after transfection, the cells were harvested and subjected to a luciferase assay. Luciferase activity was measured using a dual-luciferase reporter assay kit (Promega).

### RNA Extraction and qRT-PCR

Total RNA was extracted from cultured cells and fresh tissues using TRIzol reagent (Invitrogen). Total miRNAs were extracted using a mirVana miRNA Isolation Kit (Ambion) from paraffin-embedded OS specimens according to the manufacturer's protocol. The levels of the miRNAs and the RNU6 endogenous control were measured using TaqMan primer sets and a TaqMan microRNA Assay Kit (Life Technologies). For the expression analysis of other genes, reverse transcription (RT) and PCR were performed with a High-Capacity cDNA Reverse Transcription kit and a QuantiTect SYBR Green PCR kit (QIAGEN), respectively. The primer sequences are listed in Table S2.

### RNA Immunoprecipitation

The Ago2-flag plasmid was transfected into the indicated cells. 48 hr after transfection, the cells were subjected to the RIP assay using anti-flag antibody or IgG, as described by Keene et al.<sup>50</sup>

### Western Blot, Immunofluorescence, and Immunohistochemistry Analysis

Western blot, immunofluorescence (IF),<sup>51</sup> and immunohistochemistry (IHC)<sup>52</sup> were performed as previously described. Anti-Notch1, anti- $\beta$ -catenin, anti-p84, anti-APC, anti-GSK3 $\beta$ , anti-CK1 $\alpha$ , and anti- $\beta$ -TrCP antibodies were purchased from Abcam. Anti-Nanog, anti-BMI1, anti-Oct4, and anti-HES1 antibodies were obtained from Cell Signaling Technologies. Anti-TET3 and anti-actin antibodies were purchased from GeneTex and Sigma, respectively. Western band intensity was quantified using ImageJ software (NIH).

### Statistical Analysis

The survival rate was calculated using the Kaplan-Meier method. Univariate and multivariate survival analyses were performed using Cox regression analysis. The  $\chi^2$  test was used to analyze the relationship between the expression levels of miR-135b and target genes. Differences between groups were determined by unpaired Student's *t* test or one-way ANOVA using the SAS statistical software package version 6.12 (SAS Institute). A *p* value <0.05 was considered statistically significant.

### SUPPLEMENTAL INFORMATION

Supplemental Information includes five figures and three tables and can be found with this article online at <http://dx.doi.org/10.1016/j.omtn.2017.06.008>.

### AUTHOR CONTRIBUTIONS

H.J. and C.-X.X. designed the experiments and wrote the paper; H.J., S.L., and Y.W. performed experiments; all authors analyzed the data; Q.-Y.T., Z.-Z.Y., Y.W., and D.W. provided reagents.

### CONFLICTS OF INTEREST

There are no conflicts of interest to disclose.

### ACKNOWLEDGMENTS

This work was supported by the National Natural Science Foundation of China (grant 81402216 to M.X. and grant 81672657 to C.-X.X.), Beijing New-star Plan of Science and Technology (grant Z14110700181409 to M.X.), and Startup Fund for Talented Scholars of Daping Hospital and Research Institute of Surgery, Third Military Medical University (to C.-X.X. and H.J.).

### REFERENCES

- Messerschmitt, P.J., Garcia, R.M., Abdul-Karim, F.W., Greenfield, E.M., and Getty, P.J. (2009). Osteosarcoma. *J. Am. Acad. Orthop. Surg.* 17, 515–527.
- Broadhead, M.L., Clark, J.C., Myers, D.E., Dass, C.R., and Choong, P.F. (2011). The molecular pathogenesis of osteosarcoma: a review. *Sarcoma* 2011, 959248.
- PosthumaDeBoer, J., Witlox, M.A., Kaspers, G.J., and van Royen, B.J. (2011). Molecular alterations as target for therapy in metastatic osteosarcoma: a review of literature. *Clin. Exp. Metastasis* 28, 493–503.
- Bielack, S.S., Kempf-Bielack, B., Branscheid, D., Carrle, D., Friedel, G., Helmke, K., Kevric, M., Jundt, G., Kühne, T., Maas, R., et al. (2009). Second and subsequent recurrences of osteosarcoma: presentation, treatment, and outcomes of 249 consecutive cooperative osteosarcoma study group patients. *J. Clin. Oncol.* 27, 557–565.
- Daw, N.C., Chou, A.J., Jaffe, N., Rao, B.N., Billups, C.A., Rodriguez-Galindo, C., Meyers, P.A., and Huh, W.W. (2015). Recurrent osteosarcoma with a single pulmonary metastasis: a multi-institutional review. *Br. J. Cancer* 112, 278–282.
- Kempf-Bielack, B., Bielack, S.S., Jürgens, H., Branscheid, D., Berdel, W.E., Exner, G.U., Göbel, U., Helmke, K., Jundt, G., Kabisch, H., et al. (2005). Osteosarcoma relapse after combined modality therapy: an analysis of unselected patients in the Cooperative Osteosarcoma Study Group (COSS). *J. Clin. Oncol.* 23, 559–568.
- Marina, N., Gebhardt, M., Teot, L., and Gorlick, R. (2004). Biology and therapeutic advances for pediatric osteosarcoma. *Oncologist* 9, 422–441.
- Du, L., Rao, G., Wang, H., Li, B., Tian, W., Cui, J., He, L., Laffin, B., Tian, X., Hao, C., et al. (2013). CD44-positive cancer stem cells expressing cellular prion protein contribute to metastatic capacity in colorectal cancer. *Cancer Res.* 73, 2682–2694.
- Iliopoulos, D., Lindahl-Alten, M., Polytyrchou, C., Hirsch, H.A., Tschlis, P.N., and Struhl, K. (2010). Loss of miR-200 inhibition of Suz12 leads to polycomb-mediated repression required for the formation and maintenance of cancer stem cells. *Mol. Cell* 39, 761–772.
- Gonçalves, C., Martins-Neves, S.R., Paiva-Oliveira, D., Oliveira, V.E., Fontes-Ribeiro, C., and Gomes, C.M. (2015). Sensitizing osteosarcoma stem cells to doxorubicin-induced apoptosis through retention of doxorubicin and modulation of apoptotic-related proteins. *Life Sci.* 130, 47–56.
- Martins-Neves, S.R., Lopes, A.O., do Carmo, A., Paiva, A.A., Simões, P.C., Abrunhosa, A.J., and Gomes, C.M. (2012). Therapeutic implications of an enriched cancer stem-like cell population in a human osteosarcoma cell line. *BMC Cancer* 12, 139.
- Tirino, V., Desiderio, V., Paino, F., De Rosa, A., Papaccio, F., Fazioli, F., Pirozzi, G., and Papaccio, G. (2011). Human primary bone sarcomas contain CD133+ cancer stem cells displaying high tumorigenicity in vivo. *FASEB J.* 25, 2022–2030.
- Wang, Y., and Teng, J.S. (2016). Increased multi-drug resistance and reduced apoptosis in osteosarcoma side population cells are crucial factors for tumor recurrence. *Exp. Ther. Med.* 12, 81–86.
- Xu, M., Jin, H., Xu, C.X., Sun, B., Song, Z.G., Bi, W.Z., and Wang, Y. (2015). miR-382 inhibits osteosarcoma metastasis and relapse by targeting Y box-binding protein 1. *Mol. Ther.* 23, 89–98.
- Fang, L., Cai, J., Chen, B., Wu, S., Li, R., Xu, X., Yang, Y., Guan, H., Zhu, X., Zhang, L., et al. (2015). Aberrantly expressed miR-582-3p maintains lung cancer stem cell-like traits by activating Wnt/ $\beta$ -catenin signalling. *Nat. Commun.* 6, 8640.

16. Yu, L., Fan, Z., Fang, S., Yang, J., Gao, T., Simões, B.M., Eyre, R., Guo, W., and Clarke, R.B. (2016). Cisplatin selects for stem-like cells in osteosarcoma by activating Notch signaling. *Oncotarget* 7, 33055–33068.
17. Yan, G.N., Lv, Y.F., and Guo, Q.N. (2016). Advances in osteosarcoma stem cell research and opportunities for novel therapeutic targets. *Cancer Lett.* 370, 268–274.
18. Martins-Neves, S.R., Paiva-Oliveira, D.I., Wijers-Koster, P.M., Abrunhosa, A.J., Fontes-Ribeiro, C., Bovée, J.V.M.G., Cleton-Jansen, A.M., and Gomes, C.M. (2016). Chemotherapy induces stemness in osteosarcoma cells through activation of Wnt/ $\beta$ -catenin signaling. *Cancer Lett.* 370, 286–295.
19. Tang, Q.L., Zhao, Z.Q., Li, J.C., Liang, Y., Yin, J.Q., Zou, C.Y., Xie, X.B., Zeng, Y.X., Shen, J.N., Kang, T., and Wang, J. (2011). Salinomycin inhibits osteosarcoma by targeting its tumor stem cells. *Cancer Lett.* 311, 113–121.
20. Martins-Neves, S.R., Corver, W.E., Paiva-Oliveira, D.I., van den Akker, B.E.W.M., Briaire-de-Brujin, I.H., Bovée, J.V.M.G., Gomes, C.M., and Cleton-Jansen, A.M. (2016). Osteosarcoma stem cells have active Wnt/ $\beta$ -catenin and overexpress SOX2 and KLF4. *J. Cell. Physiol.* 231, 876–886.
21. Wang, R., Sun, Q., Wang, P., Liu, M., Xiong, S., Luo, J., Huang, H., Du, Q., Geller, D.A., and Cheng, B. (2016). Notch and Wnt/ $\beta$ -catenin signaling pathway play important roles in activating liver cancer stem cells. *Oncotarget* 7, 5754–5768.
22. Garzon, R., Calin, G.A., and Croce, C.M. (2009). MicroRNAs in cancer. *Annu. Rev. Med.* 60, 167–179.
23. Bu, P., Chen, K.Y., Chen, J.H., Wang, L., Walters, J., Shin, Y.J., Goerger, J.P., Sun, J., Witherspoon, M., Rakhilin, N., et al. (2013). A microRNA miR-34a-regulated bimodal switch targets Notch in colon cancer stem cells. *Cell Stem Cell* 12, 602–615.
24. Zhao, J.J., Lin, J., Zhu, D., Wang, X., Brooks, D., Chen, M., Chu, Z.B., Takada, K., Ciccarelli, B., Admin, S., et al. (2014). miR-30-5p functions as a tumor suppressor and novel therapeutic tool by targeting the oncogenic Wnt/ $\beta$ -catenin/BCL9 pathway. *Cancer Res.* 74, 1801–1813.
25. Pei, H., Jin, Z., Chen, S., Sun, X., Yu, J., and Guo, W. (2015). MiR-135b promotes proliferation and invasion of osteosarcoma cells via targeting FOXO1. *Mol. Cell. Biochem.* 400, 245–252.
26. Matsuyama, H., Suzuki, H.I., Nishimori, H., Noguchi, M., Yao, T., Komatsu, N., Mano, H., Sugimoto, K., and Miyazono, K. (2011). miR-135b mediates NPM-ALK-driven oncogenicity and renders IL-17-producing immunophenotype to anaplastic large cell lymphoma. *Blood* 118, 6881–6892.
27. Yang, X., Wang, X., Nie, F., Liu, T., Yu, X., Wang, H., Li, Q., Peng, R., Mao, Z., Zhou, Q., and Li, G. (2015). miR-135 family members mediate podocyte injury through the activation of Wnt/ $\beta$ -catenin signaling. *Int. J. Mol. Med.* 36, 669–677.
28. Tu, X., Delgado-Calle, J., Condon, K.W., Maycas, M., Zhang, H., Carlesso, N., Taketo, M.M., Burr, D.B., Plotkin, L.I., and Bellido, T. (2015). Osteocytes mediate the anabolic actions of canonical Wnt/ $\beta$ -catenin signaling in bone. *Proc. Natl. Acad. Sci. USA* 112, E478–E486.
29. O'Brien, C.A., Kreso, A., and Jamieson, C.H. (2010). Cancer stem cells and self-renewal. *Clin. Cancer Res.* 16, 3113–3120.
30. Visvader, J.E., and Lindeman, G.J. (2008). Cancer stem cells in solid tumours: accumulating evidence and unresolved questions. *Nat. Rev. Cancer* 8, 755–768.
31. Rodilla, V., Villanueva, A., Obrador-Hevia, A., Robert-Moreno, A., Fernández-Majada, V., Grilli, A., López-Bigas, N., Bellora, N., Albà, M.M., Torres, F., et al. (2009). Jagged1 is the pathological link between Wnt and Notch pathways in colorectal cancer. *Proc. Natl. Acad. Sci. USA* 106, 6315–6320.
32. Song, S.J., Polisenio, L., Song, M.S., Ala, U., Webster, K., Ng, C., Beringer, G., Brikbak, N.J., Yuan, X., Cantley, L.C., et al. (2013). MicroRNA-antagonism regulates breast cancer stemness and metastasis via TET-family-dependent chromatin remodeling. *Cell* 154, 311–324.
33. Brabletz, S., Bajdak, K., Meidhof, S., Burk, U., Niedermann, G., Firat, E., Wellner, U., Dimmler, A., Faller, G., Schubert, J., and Brabletz, T. (2011). The ZEB1/miR-200 feedback loop controls Notch signalling in cancer cells. *EMBO J.* 30, 770–782.
34. Valeri, N., Braconi, C., Gasparini, P., Murgia, C., Lampis, A., Paulus-Hock, V., Hart, J.R., Ueno, L., Grivnikov, S.I., Lovat, F., et al. (2014). MicroRNA-135b promotes cancer progression by acting as a downstream effector of oncogenic pathways in colon cancer. *Cancer Cell* 25, 469–483.
35. Lowery, A.J., Miller, N., Devaney, A., McNeill, R.E., Davoren, P.A., Lemetre, C., Benes, V., Schmidt, S., Blake, J., Ball, G., and Kerin, M.J. (2009). MicroRNA signatures predict oestrogen receptor, progesterone receptor and HER2/neu receptor status in breast cancer. *Breast Cancer Res.* 11, R27.
36. Lulla, R.R., Costa, F.F., Bischof, J.M., Chou, P.M., de F Bonaldo, M., Vanin, E.F., and Soares, M.B. (2011). Identification of differentially expressed microRNAs in osteosarcoma. *Sarcoma* 2011, 732690.
37. Wang, G., Wang, Y., Feng, W., Wang, X., Yang, J.Y., Zhao, Y., Wang, Y., and Liu, Y. (2008). Transcription factor and microRNA regulation in androgen-dependent and -independent prostate cancer cells. *BMC Genomics* 9 (Suppl 2), S22.
38. Lin, C.W., Chang, Y.L., Chang, Y.C., Lin, J.C., Chen, C.C., Pan, S.H., Wu, C.T., Chen, H.Y., Yang, S.C., Hong, T.M., and Yang, P.C. (2013). MicroRNA-135b promotes lung cancer metastasis by regulating multiple targets in the Hippo pathway and LZTS1. *Nat. Commun.* 4, 1877.
39. Engin, F., Bertin, T., Ma, O., Jiang, M.M., Wang, L., Sutton, R.E., Donehower, L.A., and Lee, B. (2009). Notch signaling contributes to the pathogenesis of human osteosarcomas. *Hum. Mol. Genet.* 18, 1464–1470.
40. Lu, Y., Guan, G.F., Chen, J., Hu, B., Sun, C., Ma, Q., Wen, Y.H., Qiu, X.C., and Zhou, Y. (2015). Aberrant CXCR4 and  $\beta$ -catenin expression in osteosarcoma correlates with patient survival. *Oncol. Lett.* 10, 2123–2129.
41. Xiao, S., Yang, Z., Lv, R., Zhao, J., Wu, M., Liao, Y., and Liu, Q. (2014). miR-135b contributes to the radioresistance by targeting GSK3 $\beta$  in human glioblastoma multiforme cells. *PLoS ONE* 9, e108810.
42. Cui, Q., Yang, S., Ye, P., Tian, E., Sun, G., Zhou, J., Sun, G., Liu, X., Chen, C., Murai, K., et al. (2016). Downregulation of TLX induces TET3 expression and inhibits glioblastoma stem cell self-renewal and tumorigenesis. *Nat. Commun.* 7, 10637.
43. Dean, M., Fojo, T., and Bates, S. (2005). Tumour stem cells and drug resistance. *Nat. Rev. Cancer* 5, 275–284.
44. Takebe, N., Harris, P.J., Warren, R.Q., and Ivy, S.P. (2011). Targeting cancer stem cells by inhibiting Wnt, Notch, and Hedgehog pathways. *Nat. Rev. Clin. Oncol.* 8, 97–106.
45. Takahashi-Yanaga, F., and Kahn, M. (2010). Targeting Wnt signaling: can we safely eradicate cancer stem cells? *Clin. Cancer Res.* 16, 3153–3162.
46. Takebe, N., Miele, L., Harris, P.J., Jeong, W., Bando, H., Kahn, M., Yang, S.X., and Ivy, S.P. (2015). Targeting Notch, Hedgehog, and Wnt pathways in cancer stem cells: clinical update. *Nat. Rev. Clin. Oncol.* 12, 445–464.
47. Okuhashi, Y., Itoh, M., Nara, N., and Tohda, S. (2011). Effects of combination of notch inhibitor plus hedgehog inhibitor or Wnt inhibitor on growth of leukemia cells. *Anticancer Res.* 31, 893–896.
48. Ma, Y., Ren, Y., Han, E.Q., Li, H., Chen, D., Jacobs, J.J., Gitelis, S., O'Keefe, R.J., Kontinen, Y.T., Yin, G., and Li, T.F. (2013). Inhibition of the Wnt- $\beta$ -catenin and Notch signaling pathways sensitizes osteosarcoma cells to chemotherapy. *Biochem. Biophys. Res. Commun.* 431, 274–279.
49. Zhou, P., Bogacki, R., McReynolds, L., and Howley, P.M. (2000). Harnessing the ubiquitination machinery to target the degradation of specific cellular proteins. *Mol. Cell* 6, 751–756.
50. Keene, J.D., Komisarow, J.M., and Friedersdorf, M.B. (2006). RIP-Chip: the isolation and identification of mRNAs, microRNAs and protein components of ribonucleoprotein complexes from cell extracts. *Nat. Protoc.* 1, 302–307.
51. Xu, C.X., Jin, H., Chung, Y.S., Shin, J.Y., Woo, M.A., Lee, K.H., Palmos, G.N., Choi, B.D., and Cho, M.H. (2008). Chondroitin sulfate extracted from the Styela clava tunic suppresses TNF- $\alpha$ -induced expression of inflammatory factors, VCAM-1 and iNOS by blocking Akt/NF- $\kappa$ B signal in JB6 cells. *Cancer Lett.* 264, 93–100.
52. Xu, M., Xu, C.X., Bi, W.Z., Song, Z.G., Jia, J.P., Chai, W., Zhang, L.H., and Wang, Y. (2013). Effects of endostar combined multidrug chemotherapy in osteosarcoma. *Bone* 57, 111–115.